Title

Extracellular free water elevations are associated with brain volume and maternal cytokine response in a longitudinal nonhuman primate maternal immune activation model

Journal

Molecular Psychiatry, 28(10)

ISSN

1359-4184

Authors

Lesh, Tyler A

Iosif, Ana-Maria

Tanase, Costin

et al.

Publication Date

2023-10-01

DOI

10.1038/s41380-023-02213-w

Peer reviewed

HHS Public Access

Author manuscript

Mol Psychiatry. Author manuscript; available in PMC 2024 April 01.

Published in final edited form as:

Mol Psychiatry. 2023 October ; 28(10): 4185–4194. doi:10.1038/s41380-023-02213-w.

Extracellular Free Water Elevations are Associated with Brain Volume and Maternal Cytokine Response in a Longitudinal Nonhuman Primate Maternal Immune Activation Model

Tyler A. Lesh[1], **Ana-Maria Iosif**[2], **Costin Tanase**[1], **Roza M. Vlasova**[3], **Amy M. Ryan**[1,4,5], **Jeffrey Bennett**[1], **Casey E. Hogrefe**[5], **Richard J. Maddock**[1], **Daniel H. Geschwind**[6], **Judy Van de Water**[4,7], **A. Kimberley McAllister**[4,8], **Martin A. Styner**[3], **Melissa D. Bauman**[1,4,5], **Cameron S. Carter**[1]

[1]Department of Psychiatry and Behavioral Sciences, University of California, Davis

[2]Division of Biostatistics, Department of Public Health Sciences, University of California, Davis

[3]Department of Psychiatry, University of North Carolina

[4]MIND Institute, University of California, Davis

[5]California National Primate Research Center

[6]Neurogenetics Program, Department of Neurology, University of California, Los Angeles

[7]Rheumatology/Allergy and Clinical Immunology, University of California, Davis

[8]Center for Neuroscience, University of California, Davis

Abstract

Maternal infection has emerged as an important environmental risk factor for neurodevelopmental disorders, including schizophrenia and autism spectrum disorders. Animal model systems of maternal immune activation (MIA) suggest that the maternal immune response plays a significant role in the offspring's neurodevelopment and behavioral outcomes. Extracellular free water is a measure of freely diffusing water in the brain that may be associated with neuroinflammation and impacted by MIA. The present study evaluates the brain diffusion characteristics of male rhesus monkeys (*Macaca mulatta*) born to MIA-exposed dams (n=14) treated with a modified form of the viral mimic polyinosinic:polycytidylic acid at the end of the first trimester. Control dams received saline injections at the end of the first trimester (n=10) or were untreated (n=4). Offspring underwent diffusion MRI scans at 6, 12, 24, 36, and 45 months. Offspring born to MIA-exposed

Corresponding author: Cameron S. Carter, M.D., 4701 X Street, Sacramento, CA 95817, Phone: 916-734-7783, Fax: 916-734-8750, cscarter@ucdavis.edu.

Statement of Author Contributions

T.A.L. contributed to study design, performed diffusion neuroimaging analyses, and wrote the majority of the manuscript. C.S.C as the grant principal investigator contributed to study design, edited, and reviewed the manuscript. A.I. performed statistical analyses, manuscript writing, and manuscript review. C.T. and R.V. contributed to data analysis of diffusion and structural data as well as manuscript review. A.M.R., C.H., and J.L.B. were involved in NHP husbandry, NHP measurement and monitoring, NHP scanning, as well as manuscript review. R.M, D.H.G, A.K.M, and M.S. contributed to study design and reviewed the manuscript. J.V.W contributed to study design, processed and measured cytokine data, and reviewed the manuscript. M.D.B. contributed to study design, oversaw the entirety of NHP husbandry, housing, and measurement, and reviewed the manuscript.

Conflicts of Interest

The authors report no competing financial interests or potential conflicts of interest.

dams showed significantly increased extracellular free water in cingulate cortex gray matter starting as early as 6 months of age and persisting through 45 months. Additionally, offspring gray matter free water in this region was significantly correlated with the magnitude of the maternal IL-6 response in the MIA-exposed dams. Significant correlations between brain volume and extracellular free water in the MIA-exposed offspring also indicate converging, multimodal evidence of the impact of MIA on brain development. These findings provide strong evidence for the construct validity of the nonhuman primate MIA model as a system of relevance for investigating the pathophysiology of human neurodevelopmental psychiatric disorders. Elevated free water in individuals exposed to immune activation in utero could represent an early marker of a perturbed or vulnerable neurodevelopmental trajectory.

Introduction

A significant body of evidence implicates maternal infection as one of the most important environmental risk factors for neurodevelopmental disorders, including schizophrenia and autism spectrum disorders [1–6]. Additional evidence implicating neuroimmune mechanisms in neurodevelopmental disorders include genetic links to the major histocompatibility complex, which contains genes that are critical for adaptive immune function [7], and alterations in measures of immune function, such as serum cytokines and chemokines, that have been repeatedly observed in schizophrenia, bipolar disorder, and autism spectrum disorder [5, 8–12].

Given the critical role that neuroimmune mechanisms play in many aspects of normal brain development and healthy synaptic function, these findings have prompted interest in developing preclinical models that can offer better insight into the mechanism by which exposure to these inflammatory factors may increase the risk for neurodevelopmental disorders [13, 14]. A large body of evidence from preclinical research using the maternal immune activation (MIA) model suggests that the maternal immune response is the critical link between exposure to a variety of viral and bacterial infections during pregnancy and alterations in fetal brain development [15–22]. In the MIA model, dams are exposed to an immune-activating agent during pregnancy, which prompts an immune response and initiates a trajectory of atypical offspring neurodevelopment reflected in altered behavior, brain structure, and function in a proportion of offspring. Rodent MIA models manifest a wide range of behavioral and neuroanatomical phenotypes suggesting that prenatal immune challenge may serve as a “disease primer” that, in combination with other genetic or environmental factors, may alter neurodevelopmental trajectories [17, 23, 24]. While comparisons between animal models and clinical disorders must be made with caution, MIA-exposed offspring do exhibit changes relevant to psychotic and autism spectrum disorders, including altered sensorimotor gating, reduced social behaviors, reduced working memory, increased sensitivity to dopamine receptor agonists, and reductions in cortical gray matter [5, 25]. Alterations in fractional anisotropy (FA) have also been identified in MIA-exposed juvenile [26] and adult [27] mice undergoing diffusion MRI. An important recent development in the investigation of neuroimmune mechanisms of altered neurodevelopment is the emergence of a nonhuman primate (NHP) MIA model. This model offers unique advantages due to the increased similarity to human brain structure and function, cognition,

and social behavior [28]. Initial studies using the NHP MIA model revealed changes in species-typical behavioral development [29, 30] and long-term alterations in the immune responses of offspring born to MIA-exposed dams [31]. Weir and colleagues [32] noted evidence of neuropathology in these offspring, which showed reductions in the diameter of apical dendrites in the dorsolateral prefrontal cortex at 3.5–4 years of age (late adolescence) that has been recently replicated in a larger cohort of MIA-exposed NHPs [33]. We have previously reported decreased frontal gray and white matter paired with subtle cognitive impairments in the present cohort of MIA-exposed rhesus monkeys that have undergone longitudinal brain and behavior phenotyping [34]. Rhesus macaque offspring exposed to influenza in utero have also been shown to exhibit subtle behavioral changes in early development and reduced overall gray matter, with the most significant reductions in the cingulate and parietal cortex [35]. Collectively, these studies suggest that rhesus monkeys prenatally exposed to immune challenge exhibit relatively normal patterns of early behavioral development despite atypical brain growth and immune system development. However, behavioral changes may become more pronounced as they approach puberty, a time that coincides with a sensitive period of neuronal reorganization and plasticity [36]. Work by our group [37] using [^{18}F]fluoro-l-m-tyrosine (FMT) positron emission tomography (PET) also reveals that adolescent MIA-exposed offspring from a separate cohort show elevations in striatal dopamine.

Maternal inflammation (i.e., maternal IL-6) has been shown to have strong associations with altered diffusion characteristics, particularly altered FA in human neonates[38]. Alterations in FA have also been regularly found in individuals with psychiatric disorders, including psychotic and autism spectrum disorders[39–42], although newer multi-shell diffusion imaging methods offer a more detailed analysis of these neuroanatomical alterations. Pasternak and colleagues previously demonstrated the utility of measuring extracellular free water as a method of adjusting for free water in calculating fractional anisotropy [43], and also as a distinct biomarker that may be associated with inflammation. This and work from our group [44, 45] have shown a pattern of increased free water and comparable free water-corrected FA in first-episode psychosis samples. In contrast, chronic samples appear to show more prominent reductions in FA [46]. In addition, results of recent back-translational work in a MIA-exposed rat model [47] show increased extracellular free water in the white matter, particularly within the corpus callosum, external capsule, and striatum. However, the effect of MIA on extracellular free water in the nonhuman primate model has never been examined and offers a greater neuroanatomical and behavioral similarity to human samples.

The goal of the present study is to use brain diffusion characteristics in NHP offspring over the first four years of life to test the hypothesis that offspring of MIA-exposed dams will show higher extracellular free water in gray matter and specifically frontal and cingulate cortex. Tissue-specific FA (FA-t) will also be examined but is hypothesized to be less significantly impacted. Finally, we anticipate that maternal immune reactivity, measured by the peak IL-6 response after injection, will be positively associated with offspring free water measures.

Materials and Methods

Experimental procedures were developed in collaboration with the veterinary, animal husbandry, and environmental enrichment staff at the California National Primate Research Center (CNPRC) and approved by the University of California, Davis Institutional Animal Care and Use Committee. All attempts were made to promote the psychological well-being of the animals participating in this research. These efforts included social housing, an enriched diet, positive reinforcement strategies, and minimizing the duration of daily training/testing sessions.

Animal Selection and MIA Procedures

Animals in this study represent the same cohort reported by Vlasova and colleagues[34]. Consequently, we present some of the methods in a condensed form. Pregnant dams between five and twelve years of age were selected (based on age, weight, parity, and the number of live births) from the indoor time-mated breeding colony at the CNPRC and assigned to MIA (n=14) and control (n=10 saline-treated and n=4 untreated) groups. Synthetic double-stranded RNA (polyinosinic:polycytidylic acid [Poly IC] stabilized with poly-L-lysine [Poly ICLC]) (Oncovir, Inc.; 0.25 mg/kg i.v.) or sterile saline (equivalent volume to Poly ICLC) was injected at 07:30 hours in the cephalic vein in awake animals on gestational day (GD) 43, 44, and 46. Blood samples collected 6 hours after the second (GD 44) and third (GD 46) Poly ICLC injections confirmed a strong pro-inflammatory cytokine response as indexed by the change in IL-6 from baseline samples as described in Vlasova et al. 2021 [34]. Following recent guideline recommendations for improving the reporting of MIA model methods, the checklist from Kentner and colleagues [48] is provided as supplementary material. One offspring from the MIA group was euthanized at 6 months of age due to an unrelated health issue and is not included in any free water analyses. A second animal from the MIA group was euthanized at 42 months of age due to an unrelated health condition and therefore does not contribute data at the final timepoint and is not included in the IL-6 correlation but is included in longitudinal free water analyses.

Rearing Conditions and Husbandry

Infants were raised in individual cages with their mothers, where they had visual access to other mother-infant pairs at all times. For 3 hours each day, one familiar adult male and four familiar mother-infant pairs were allowed to freely interact in a large cage (3 m long x 1.8 m wide x 2 m high) to provide enrichment and facilitate species-typical social development. The infants were weaned from their mothers at 6 months of age and were continuously paired with a familiar peer from their rearing group. Weanlings continued the same group socialization routine, with the addition of a non-related adult female, through approximately 18 months of age and remained with treatment-matched permanent pairs thereafter. In addition to the longitudinal neuroimaging studies, the offspring participated in behavioral testing paradigms throughout development, as described in Vlasova et al. [34].

Neuroimaging

Magnetic resonance images were collected at 6, 12, 24, 36, and 45 months of age using a Siemens Magnetom Skyra 3-T (Davis, California) with an 8-channel coil optimized for

nonhuman primate brain scanning (RapidMR, Columbus, Ohio). While twenty-four animals were also scanned at one month of age (and three animals at three months), poor image quality and low gray/white T1 image contrast prevented analysis for the present study. Animals were sedated with ketamine for intubation and then anesthetized with isoflurane (1.3–2.0%) at varying rates to maintain a steady state of anesthesia. Respiration and heart rate were continually monitored throughout imaging by trained CNPRC staff. Two animals showed sensitivity to isoflurane and were consequently sedated with propofol at subsequent time points. A third animal initially showed isoflurane sensitivity and received propofol for the six-month scan but was tested and cleared to receive isoflurane for the remaining time points. Once the animal was placed in and centered at the mid-line of the MR-compatible stereotaxic frame, the 8-channel receiver coil was attached to the stereotaxic frame using a custom connector. The center point of the 8-channel coil was positioned at AP+10 on the stereotaxic frame, and the Skyra table was then "landmarked" at AP+10 on the stereotaxic frame so that the center of the animal's brain was at isocenter. Fluids were maintained with saline at a rate of 10 ml/kg/hr for the duration of the MRI scan.

Acquisition Parameters: T1 weighted images (480 sagittal slices) were acquired with TR=2500 ms, TE=3.65 msec, flip angle=7°, field of view 256×256, voxel size during acquisition was 0.6×0.6×0.6 mm which was interpolated during image reconstruction in the scanner to 512×512 voxels with a resolution of 0.3×0.3×0.3 mm. Diffusion data were acquired with the following settings: TR=5600-msec, echo time=90 msec, 0.7 mm in-plane resolution, and 42 slices at 1.4 mm slice thickness. The sequence included 64 directions acquired F-H with the following b-shells: 11 x b=0, 23 x b=500, 22 x b=900, 19 x b=1400. Additional b=0 images were collected in the opposing phase encoding direction to correct for susceptibility-induced distortion.

Image processing: All images were processed without knowledge of group assignment and only with knowledge of age at scan. T1 weighted images were aligned to a common atlas [49], bias field corrected, and brain masked using AutoSeg_3.3.2 [50]. Brain masks were manually corrected if necessary. Following this preprocessing, T1 weighted images were segmented into gray matter (GM), white matter (WM), and cerebrospinal fluid (CSF) using NeosegPipeline_v1.0.8 [51]. The University of North Carolina lobar parcellation (https://www.nitrc.org/projects/unc_macaque/) [52] was employed to parcellate the tissue segmentations into 24 lobar brain regions using the multi-atlas fusion in AutoSeg_3.3.2 [50]. All segmentation and parcellation results were visually quality controlled.

Diffusion images were thoroughly inspected visually for artifacts, and DTIPrep [53] was used to identify slice-wise, interlace-wise, and gradient-wise intensity artifacts. Images with artifacts were discarded, and the remaining underwent susceptibility-induced distortion correction using opposite phase encoding b=0 images and the FSL topup tool [54, 55]. Data were corrected for eddy currents and realigned using FSL eddy [56], including rotation of b-matrices. The Dipy diffusion imaging library [57] and included free water elimination model [58] were used to calculate all diffusion metrics. This model expands the typical DTI model and assumes that each voxel contains two components: an anisotropic tissue-bound component and an isotropic extracellular free water component. In this study, we evaluated

both the free water component and tissue-specific fractional anisotropy (FA-t), which reflects traditional FA with the free water component eliminated. To align diffusion data with the segmented and parcellated regions of interest, fully processed mean b=0 images were nonlinearly warped to each individual animal's T2-weighted image using Advanced Neuroimaging Tools (ANTs) SyN [59, 60]. This nonlinear transformation was then applied to each animal's free water and FA-t images to bring the diffusion measures into the same space as the segmented and parcellated regions of interest. As suggested by the Dipy toolbox, we thresholded FA-t and free water output to remove voxels with greater than 70% free water, which limits artifacts caused by voxels with large free water fractions (i.e., voxels containing largely cerebrospinal fluid). The code used to process data presented in this manuscript are publicly available (https://github.com/NIRALUser and https://github.com/TCANLab/NHPfwtools), and measurement data are shared at the NHPfwtools repository as well.

Figure 1 depicts the a priori regions of interest (ROI) that were selected (whole-brain, prefrontal, frontal, cingulate, and temporal limbic) based on the body of literature highlighting neuroanatomical alterations associated with MIA [61–64]. Free water was examined separately in white and gray matter ROIs and FA-t was examined only in the white matter of each ROI.

Statistical analysis

Statistical analysis employed linear mixed-effects models [65] to model free water measures trajectories and to evaluate group differences between 6 and 45 months of age. An advantage of this approach is the ability to use all available data for an individual, to account for the effect of covariates of interest, and to model heterogeneous variances (across groups or time). Outcomes were white and gray matter free water (FW) and FA-t in whole-brain, prefrontal, frontal, cingulate, and temporal limbic regions. Separate models were fitted for each ROI, and to aid model convergence, all outcomes were rescaled by multiplying with 100. A fourth-order orthogonal polynomial model was sufficiently complex to describe all the outcomes in our data adequately. Orthogonal polynomials are transformations of natural polynomials that make the individual terms independent (i.e., remove the correlation between, for example, linear and quadratic age), thus allowing for a more precise evaluation of differences in free water trajectories. We accounted for within-subject correlation due to the repeatedly measured outcomes using a random intercept and random slopes for the linear up to quadratic trends. We followed a two-step process to identify the best-fitting model for each outcome. We first selected the covariance structure that was the most appropriate, using a model that included fixed effects for the group (MIA vs. control), linear, quadratic, cubic, and quartic orthogonal polynomials for age at scan (measured in years), and all the interactions between group and polynomial effects of age. In the second step, we examined whether models with higher-degree polynomials and interactions provided a better fit than simpler models. We sequentially removed the highest degree polynomial and interaction terms and compared all resulting models to identify the model with the lowest corrected Akaike information criterion (AIC) [66, 67]. The corrected AIC (a finite-sample corrected version of AIC) is a measure of overall model fit, penalized for the number of predictors to avoid overfitting. The performance of models was considered similar if the difference

in corrected AICs was smaller than 2. In cases where the performance of two models was similar, we also examined the Bayesian information criterion (BIC) [68], and we confirmed that the reported model also had a lower BIC. All models were validated both graphically and analytically. Tests were two-sided, with $\alpha = 0.05$. All analyses were conducted in SAS version 9.4. (SAS Institute Inc., Cary, NC).

Results

MIA Effect and Developmental Trajectories

As reported by Vlasova and colleagues [34], blood samples revealed a strong increase in IL-6 levels from baseline in MIA-exposed dams compared to saline controls (Figure 2). Additionally, there were no significant differences between groups in any gross measure of offspring development, including growth trajectories (weight, crown-rump, head circumference), neuromotor reflexes, and overall health. However, the MIA-exposed offspring in this study showed measurable cognitive deficits that were selective to tasks requiring high levels of sustained attention and cognitive flexibility, beginning at 18 months of age [34].

Neuroimaging Results

Assessment of diffusion data after quality control procedures revealed an average of 3.3 volumes (range of 0 to 18) were discarded per animal. Importantly, the number of discarded images did not differ between treatment groups (p=0.64), and there was no significant interaction with time (p=0.62). A significant main effect of time was noted, with more volumes discarded at later time points in both groups (p<0.001). An example image of the type of artifacts that were identified and led to discarded data is presented in the supplement (Figure S1).

Summary information for all diffusion measures and regions of interest is presented in Table 1, and results of the best-fitting statistical models are summarized in Table 2. None of the models revealed group-by-age interactions. Free water ROI analyses revealed a significant main effect of group and age in the cingulate gray matter (Figure 3), with higher free water in the MIA offspring than in controls and higher free water over time. Other regions of interest showed only significant effects of age. ROI analyses of FA-t in white matter revealed only significant effects of age, with no main effects of group. For ease of viewing these patterns, estimated effect sizes for the group differences were calculated using mixed-effects models [69] and displayed in the supplement (Figure S2).

To evaluate whether the magnitude of the maternal immune response played a role in developmental changes in diffusion characteristics of the offspring, we computed Spearman's rank correlations between summaries reflecting relevant and interpretable aspects of IL-6 and FW data. Maternal IL-6 response was summarized by the peak level (i.e., the maximum) after the second and third injections, which may be interpreted as the maximum effect of the injection. Free water in ROIs where a significant free water group effect was identified was summarized by calculating the area under the curve for each individual trajectory, standardized by the length in the study. This approach was

preferable to averaging because the imaging was performed at unequal time intervals, and there was a slight variation in the ages at the scan across offspring. These correlations were conducted separately in the two groups, using only the animals who had complete data (12 MIA, 10 Control). As shown in Figure 4, free water and maternal IL-6 reactivity were significantly correlated in cingulate gray matter (Spearman's ρ=0.71, p=0.01) in the MIA-exposed offspring, but not the control group (ρ=.02, p=0.96).

Given significant reductions in regional brain volume and subtle behavioral deficits noted in the same cohort by Vlasova and colleagues [34], we performed post-hoc analyses exploring the relationship between these volumetric/behavioral findings and free water. Specifically, we conducted Spearman's rank correlations between brain volume and free water within regions that showed either significant group differences in brain volume[34] (prefrontal gray, frontal gray, frontal white) or significant group free water differences (cingulate gray). Additionally, we examined the relationship between free water and brain volume in whole-brain gray and white matter. These six correlations were based on the area under the curve summaries calculated as described above for free water and brain volume. Finally, in terms of behavioral data, we focused on the relationship between cingulate gray matter free water and behavioral metrics that showed significant group differences in our previous study[34], which include CPT (Continuous Performance Task) false alarms and ID/ED (Intra/Extradimensional) miss rate.

Exploratory analyses evaluating the relationship between brain volume and free water (supplementary Table S1) revealed significant inverse associations between these measures in the MIA-exposed offspring in whole-brain, frontal, prefrontal, and cingulate gray matter as well as whole-brain white matter. One significant positive relationship was identified between free water and frontal white matter volume in the control offspring. Using Fisher r-to-z transformations to test whether the relationship between brain volume and free water was statistically stronger in one group compared to the other, we identified a significantly stronger (more negative) relationship between these measures in MIA compared to control offspring in frontal and prefrontal gray matter as well as frontal and whole-brain white matter (see Table S1 in supplement). Analyses exploring the relationship between free water and behavioral measures (CPT false alarms and ID/ED misses) revealed no significant relationships in either group (all p>0.34).

Discussion

The present study revealed, for the first time, a pattern of elevated extracellular free water in the cingulate cortex gray matter in NHP MIA offspring. Furthermore, these elevations emerged as early as 6 months in development and were stably elevated over the 4-year study period, equivalent to childhood through late adolescence. These free water alterations occurred in the absence of significant differences in white matter integrity as measured using FA-t. Furthermore, and importantly, maternal plasma IL-6 levels were significantly associated with elevated FW in the MIA offspring, providing additional evidence for a robust causal link between maternal immune response and subsequent atypical neurodevelopment.

Free water elevations have recently been reported in an MIA rat model [47]. These data parallel the present study in showing free water elevations in the absence of FA-t group differences, suggesting that MIA-induced changes in offspring may be specific to extracellular diffusion characteristics as opposed to white matter integrity per se. Di Biase and colleagues reported higher extracellular free water in the white matter, particularly within the corpus callosum, external capsule, and striatum, and did not report analyses of gray matter FW. Notably, the finding of MIA-induced FA alterations in offspring in rodent models is inconsistent. In MIA mouse models, both increases and decreases in FA have been reported depending upon the region examined and the age of the MIA offspring [26, 27, 70]. However, these studies did not account for the free water component, which should provide better specificity on how these diffusion characteristics are altered.

The present NHP MIA model provides an opportunity to explore MIA-induced free water elevations reported in rodent models in a species more closely related to humans. It has been argued from human studies that the presence of increased FW may reflect the presence of neuroinflammatory or some other neuroimmune perturbation at illness onset[44–46, 71]. However, such an interpretation is arguably indirect as other mechanisms that might lead to increased extracellular volumes in gray and white matter, such as atrophy, could also lead to this result. In an effort to address this concern, recent work by our group identified a relationship between higher free water in a first-episode schizophrenia sample and an important antioxidant and free radical buffer in the brain, glutathione [45]. This correlational analysis revealed that individuals with higher free water also showed lower glutathione levels, providing converging evidence for a measurable neuroinflammatory or neuroimmune perturbation. In addition, recent work in the rat MIA model by Di Biase and colleagues [47] identified an association between white matter extracellular free water and proinflammatory peripheral cytokine levels, providing further evidence for immune involvement. The results of the present study in the MIA nonhuman primate model provide additional support for this interpretation since manipulating the maternal immune response at a critical time during pregnancy resulted in a developmental alteration in cingulate FW in the offspring.

Finally, we recently reported an early and stable onset of reduced frontal and prefrontal brain volume in this cohort of NHP MIA offspring [34]. Our current findings of robust and novel inverse relationships between free water and brain volume in frontal, prefrontal, and cingulate gray matter in this sample offer additional insight into MIA's impact on NHP offspring brain development. Histological studies suggest that volume reductions in MIA rodent offspring may be related to reduced neuronal density, particularly of GABAergic neurons [72–75]. One driver of these reductions may be altered pyramidal neuronal migration, which has been reported in MIA offspring [72, 73, 76, 77]. In addition to neuronal count, rodent MIA models highlight reductions in synaptic density [78], although this has not been found in nonhuman primates[32]. Instead, Weir and colleagues[32] identified reduced apical dendrite diameter and an increased number of oblique dendrites recently replicated in a larger NHP MIA model cohort [33]. While we did not identify group differences in white matter free water, we did identify significant relationships between whole-brain white matter and the corresponding free water fraction, specifically in MIA offspring. Work by Richetto and colleagues in a rodent MIA model[79] highlights alterations in transcriptional and epigenetic factors related to myelin stability proteins and an MIA-driven alteration in myelin "quality"

that might inform this relationship. However, at this stage, it is difficult to disentangle whether free water increases are a consequence of altered volumetric trajectories, whether the balance of tissue-bound versus extracellular free water might contribute to neuronal morphology and structure, or rather that brain volume and free water alterations reflect the influence of a third variable and different mechanisms. Nonetheless, the fact that these relationships are mainly present in and stronger in MIA offspring compared to control offspring provides converging evidence that these measures are complementary indicators of the impact of MIA on neurodevelopment.

The finding that dams with a higher IL-6 response to poly-ICLC gave birth to offspring with higher free water in the cingulate cortex also provides a potential mechanism by which MIA may induce changes in offspring neurodevelopment. Studies in rodents have suggested that IL-6 plays a prominent role in mediating MIA-induced changes in fetal brain development and behavior [80]. Additionally, our recent work in the rodent MIA model has identified individual variation in the maternal immune response as a predictor of the severity of offspring behavioral phenotypes [81]. These data also align with work by Garay and colleagues [82] that identified increased levels of largely pro-inflammatory cytokines in the brains of MIA mice offspring, particularly in frontal and cingulate cortices. The link to human brain development has also been highlighted by Rasmussen and colleagues [38], who found that higher maternal IL-6 levels were associated with lower FA values in the uncinate fasciculus in neonates. Furthermore, developmental changes in FA were found to mediate the relationship between maternal IL-6 and infant cognition one year later. Taken together, these animal model systems and human studies highlight a robust relationship between maternal inflammation and offspring brain and behavioral development.

The present study has several limitations that must be acknowledged. As with any study involving an animal model, one must use caution in overinterpreting and ascribing direct links to a particular disorder in humans. While many characteristics of the MIA model have face validity as relevant to psychiatric disorders, such as schizophrenia (e.g., elevated striatal dopamine [83, 84], altered prepulse inhibition [80], reduced social behavior [85], and reduced prefrontal brain volume [35]), commonalities are also seen with autism spectrum disorder (e.g., repetitive behaviors and reduced social behavior [85]). The sample size is also relatively modest, and as such, we had the power to detect only moderate to large effect sizes. While we attempted to minimize the number of statistical tests by identifying a limited number of a priori regions of interest, it should be noted that we did not correct for multiple comparisons. There is also emerging evidence that sex may play an important role in MIA studies [86, 87], and the present study was limited to male offspring. Studies in a new cohort that will allow us to gain insights into possible sex differences in the nonhuman primate MIA model are currently underway.

These results, together with the anatomical results reported by Vlasova and colleagues [34], provide strong evidence for the construct validity of the NHP MIA model as a system of relevance for investigating the pathophysiology of human neurodevelopmental psychiatric disorders. Recent theories propose that activation of the immune system during pregnancy may act as a disease primer that leaves the organism vulnerable to additional environmental insults during development that may increase the risk for psychopathology. Elevated free

water in individuals exposed to immune activation in utero could represent an early marker of a perturbed or vulnerable neurodevelopmental trajectory. The current MIA NHP cohort will ultimately undergo cellular and molecular analyses of brain tissue, enabling us to shed more light on the nature of altered neurodevelopment associated with MIA and its impact on cellular and molecular mechanisms in the NHP brain.

Supplementary Material

Refer to Web version on PubMed Central for supplementary material.

Acknowledgments

These studies were supported by the UC Davis Conte Center to CSC (NIMH; P50MH106438). Development of the nonhuman primate model and behavioral characterization of the offspring were supported by (P50MH106438-04S1) to MDB. Cytokine analysis was supported by the Biological and Molecular Analysis Core of the MIND Institute Intellectual and Developmental Disabilities Research Center (P50HD103526). The authors would like to thank Dr. Thorsten Feiweier from Siemens AG, Healthcare, for providing the prototype software package for advanced diffusion imaging, which was used to acquire data in the present study. Additional support was provided by the base grant (RR00169) of the California National Primate Research Center (CNPRC). We thank the veterinary and animal services staff of the CNPRC for care for the animals. Dr. Andres Salazar, MD, Oncovir, Washington D.C, kindly provided poly ICLC.

References

1. Brown AS, Hooton J, Schaefer CA, Zhang H, Petkova E, Babulas V et al. Elevated maternal interleukin-8 levels and risk of schizophrenia in adult offspring. Am J Psychiatry 2004; 161(5): 889–895. [PubMed: 15121655]
2. Stefansson H, Ophoff RA, Steinberg S, Andreassen OA, Cichon S, Rujescu D et al. Common variants conferring risk of schizophrenia. Nature 2009; 460(7256): 744–747. [PubMed: 19571808]
3. Careaga M, Rogers S, Hansen RL, Amaral DG, Van de Water J, Ashwood P. Immune Endophenotypes in Children With Autism Spectrum Disorder. Biol Psychiatry 2017; 81(5): 434–441. [PubMed: 26493496]
4. Gonzalez-Liencres C, Tas C, Brown EC, Erdin S, Onur E, Cubukcoglu Z et al. Oxidative stress in schizophrenia: a case-control study on the effects on social cognition and neurocognition. BMC Psychiatry 2014; 14: 268. [PubMed: 25248376]
5. Brown AS, Meyer U. Maternal Immune Activation and Neuropsychiatric Illness: A Translational Research Perspective. Am J Psychiatry 2018; 175(11): 1073–1083. [PubMed: 30220221]
6. Lee Younga H., Cherkerzian Sara, Seidman Larry J., Papandonatos George D., Savitz David A., Tsuang Ming T., et al. Maternal Bacterial Infection During Pregnancy and Offspring Risk of Psychotic Disorders: Variation by Severity of Infection and Offspring Sex. American Journal of Psychiatry 2020; 177(1): 66–75. [PubMed: 31581799]
7. Sekar A, Bialas AR, de Rivera H, Davis A, Hammond TR, Kamitaki N et al. Schizophrenia risk from complex variation of complement component 4. Nature 2016; 530(7589): 177–183. [PubMed: 26814963]
8. Han VX, Patel S, Jones HF, Dale RC. Maternal immune activation and neuroinflammation in human neurodevelopmental disorders. Nat Rev Neurol 2021; 17(9): 564–579. [PubMed: 34341569]
9. Han VX, Patel S, Jones HF, Nielsen TC, Mohammad SS, Hofer MJ et al. Maternal acute and chronic inflammation in pregnancy is associated with common neurodevelopmental disorders: a systematic review. Transl Psychiatry 2021; 11(1): 71. [PubMed: 33479207]
10. Miller BJ, Buckley P, Seabolt W, Mellor A, Kirkpatrick B. Meta-analysis of cytokine alterations in schizophrenia: clinical status and antipsychotic effects. Biol Psychiatry 2011; 70(7): 663–671. [PubMed: 21641581]
11. Modabbernia A, Taslimi S, Brietzke E, Ashrafi M. Cytokine alterations in bipolar disorder: a meta-analysis of 30 studies. Biol Psychiatry 2013; 74(1): 15–25. [PubMed: 23419545]

12. Masi A, Quintana DS, Glozier N, Lloyd AR, Hickie IB, Guastella AJ. Cytokine aberrations in autism spectrum disorder: a systematic review and meta-analysis. Mol Psychiatry 2015; 20(4): 440–446. [PubMed: 24934179]
13. Estes ML, McAllister AK. Maternal immune activation: Implications for neuropsychiatric disorders. Science 2016; 353(6301): 772–777. [PubMed: 27540164]
14. Guma E, Plitman E, Chakravarty MM. The role of maternal immune activation in altering the neurodevelopmental trajectories of offspring: A translational review of neuroimaging studies with implications for autism spectrum disorder and schizophrenia. Neurosci Biobehav Rev 2019; 104: 141–157. [PubMed: 31265870]
15. Gumusoglu SB, Stevens HE. Maternal Inflammation and Neurodevelopmental Programming: A Review of Preclinical Outcomes and Implications for Translational Psychiatry. Biol Psychiatry 2019; 85(2): 107–121. [PubMed: 30318336]
16. Bergdolt L, Dunaevsky A. Brain changes in a maternal immune activation model of neurodevelopmental brain disorders. Prog Neurobiol 2019; 175: 1–19. [PubMed: 30590095]
17. Meyer U Neurodevelopmental Resilience and Susceptibility to Maternal Immune Activation. Trends Neurosci 2019; 42(11): 793–806. [PubMed: 31493924]
18. Shi L, Tu N, Patterson PH. Maternal influenza infection is likely to alter fetal brain development indirectly: the virus is not detected in the fetus. International journal of developmental neuroscience : the official journal of the International Society for Developmental Neuroscience 2005; 23(2–3): 299–305. [PubMed: 15749254]
19. Shi L, Fatemi SH, Sidwell RW, Patterson PH. Maternal influenza infection causes marked behavioral and pharmacological changes in the offspring. J Neurosci 2003; 23(1): 297–302. [PubMed: 12514227]
20. Meyer U, Feldon J, Schedlowski M, Yee BK. Immunological stress at the maternal-foetal interface: a link between neurodevelopment and adult psychopathology. Brain Behav Immun 2006; 20(4): 378–388. [PubMed: 16378711]
21. Patterson PH. Immune involvement in schizophrenia and autism: etiology, pathology and animal models. Behav Brain Res 2009; 204(2): 313–321. [PubMed: 19136031]
22. Urakubo A, Jarskog LF, Lieberman JA, Gilmore JH. Prenatal exposure to maternal infection alters cytokine expression in the placenta, amniotic fluid, and fetal brain. Schizophr Res 2001; 47(1): 27–36. [PubMed: 11163542]
23. Knuesel I, Chicha L, Britschgi M, Schobel SA, Bodmer M, Hellings JA et al. Maternal immune activation and abnormal brain development across CNS disorders. Nat Rev Neurol 2014; 10(11): 643–660. [PubMed: 25311587]
24. Guma E, Bordignon PDC, Devenyi GA, Gallino D, Anastassiadis C, Cvetkovska V et al. Early or Late Gestational Exposure to Maternal Immune Activation Alters Neurodevelopmental Trajectories in Mice: An Integrated Neuroimaging, Behavioral, and Transcriptional Study. Biol Psychiatry 2021; 90(5): 328–341. [PubMed: 34053674]
25. Meyer U, Feldon J. Epidemiology-driven neurodevelopmental animal models of schizophrenia. Prog Neurobiol 2010; 90(3): 285–326. [PubMed: 19857543]
26. Fatemi SH, Folsom TD, Reutiman TJ, Abu-Odeh D, Mori S, Huang H et al. Abnormal expression of myelination genes and alterations in white matter fractional anisotropy following prenatal viral influenza infection at E16 in mice. Schizophr Res 2009; 112(1–3): 46–53. [PubMed: 19487109]
27. Li Q, Cheung C, Wei R, Cheung V, Hui ES, You Y et al. Voxel-based analysis of postnatal white matter microstructure in mice exposed to immune challenge in early or late pregnancy. Neuroimage 2010; 52(1): 1–8. [PubMed: 20399275]
28. Ryan AM, Bauman MD. Primate Models as a Translational Tool for Understanding Prenatal Origins of Neurodevelopmental Disorders Associated With Maternal Infection. Biol Psychiatry Cogn Neurosci Neuroimaging 2022; 7(5): 510–523. [PubMed: 35276404]
29. Bauman MD, Iosif AM, Smith SE, Bregere C, Amaral DG, Patterson PH. Activation of the maternal immune system during pregnancy alters behavioral development of rhesus monkey offspring. Biol Psychiatry 2014; 75(4): 332–341. [PubMed: 24011823]

30. Machado CJ, Whitaker AM, Smith SE, Patterson PH, Bauman MD. Maternal immune activation in nonhuman primates alters social attention in juvenile offspring. Biol Psychiatry 2015; 77(9): 823–832. [PubMed: 25442006]

31. Rose DR, Careaga M, Van de Water J, McAllister K, Bauman MD, Ashwood P. Long-term altered immune responses following fetal priming in a non-human primate model of maternal immune activation. Brain Behav Immun 2017; 63: 60–70. [PubMed: 27876552]

32. Weir RK, Forghany R, Smith SE, Patterson PH, McAllister AK, Schumann CM et al. Preliminary evidence of neuropathology in nonhuman primates prenatally exposed to maternal immune activation. Brain Behav Immun 2015; 48: 139–146. [PubMed: 25816799]

33. Hanson KL, Weir RK, Iosif AM, Van de Water J, Carter CS, McAllister AK et al. Altered dendritic morphology in dorsolateral prefrontal cortex of nonhuman primates prenatally exposed to maternal immune activation. Brain Behav Immun 2023; 109: 92–101. [PubMed: 36610487]

34. Vlasova RM, Iosif AM, Ryan AM, Funk LH, Murai T, Chen S et al. Maternal Immune Activation during Pregnancy Alters Postnatal Brain Growth and Cognitive Development in Nonhuman Primate Offspring. J Neurosci 2021; 41(48): 9971–9987. [PubMed: 34607967]

35. Short SJ, Lubach GR, Karasin AI, Olsen CW, Styner M, Knickmeyer RC et al. Maternal influenza infection during pregnancy impacts postnatal brain development in the rhesus monkey. Biol Psychiatry 2010; 67(10): 965–973. [PubMed: 20079486]

36. Hoftman GD, Lewis DA. Postnatal developmental trajectories of neural circuits in the primate prefrontal cortex: identifying sensitive periods for vulnerability to schizophrenia. Schizophr Bull 2011; 37(3): 493–503. [PubMed: 21505116]

37. Bauman MD, Lesh TA, Rowland DJ, Schumann CM, Smucny J, Kukis DL et al. Preliminary evidence of increased striatal dopamine in a nonhuman primate model of maternal immune activation. Transl Psychiatry 2019; 9(1): 135. [PubMed: 30979867]

38. Rasmussen JM, Graham AM, Entringer S, Gilmore JH, Styner M, Fair DA et al. Maternal Interleukin-6 concentration during pregnancy is associated with variation in frontolimbic white matter and cognitive development in early life. Neuroimage 2019; 185: 825–835. [PubMed: 29654875]

39. Kelly S, Jahanshad N, Zalesky A, Kochunov P, Agartz I, Alloza C et al. Widespread white matter microstructural differences in schizophrenia across 4322 individuals: results from the ENIGMA Schizophrenia DTI Working Group. Mol Psychiatry 2017.

40. Andrews DS, Lee JK, Solomon M, Rogers SJ, Amaral DG, Nordahl CW. A diffusion-weighted imaging tract-based spatial statistics study of autism spectrum disorder in preschool-aged children. J Neurodev Disord 2019; 11(1): 32. [PubMed: 31839001]

41. Karlsgodt KH. Diffusion Imaging of White Matter In Schizophrenia: Progress and Future Directions. Biol Psychiatry Cogn Neurosci Neuroimaging 2016; 1(3): 209–217. [PubMed: 27453952]

42. Travers BG, Adluru N, Ennis C, Tromp do PM, Destiche D, Doran S et al. Diffusion tensor imaging in autism spectrum disorder: a review. Autism Res 2012; 5(5): 289–313. [PubMed: 22786754]

43. Pasternak O, Sochen N, Gur Y, Intrator N, Assaf Y. Free water elimination and mapping from diffusion MRI. Magn Reson Med 2009; 62(3): 717–730. [PubMed: 19623619]

44. Pasternak O, Westin CF, Bouix S, Seidman LJ, Goldstein JM, Woo TU et al. Excessive extracellular volume reveals a neurodegenerative pattern in schizophrenia onset. J Neurosci 2012; 32(48): 17365–17372. [PubMed: 23197727]

45. Lesh TA, Maddock RJ, Howell A, Wang H, Tanase C, Daniel Ragland J et al. Extracellular free water and glutathione in first-episode psychosis-a multimodal investigation of an inflammatory model for psychosis. Mol Psychiatry 2021; 26(3): 761–771. [PubMed: 31138893]

46. Pasternak O, Westin CF, Dahlben B, Bouix S, Kubicki M. The extent of diffusion MRI markers of neuroinflammation and white matter deterioration in chronic schizophrenia. Schizophr Res 2015; 161(1): 113–118. [PubMed: 25126717]

47. Di Biase MA, Katabi G, Piontkewitz Y, Cetin-Karayumak S, Weiner I, Pasternak O. Increased extracellular free-water in adult male rats following in utero exposure to maternal immune activation. Brain Behav Immun 2020; 83: 283–287. [PubMed: 31521731]

48. Kentner AC, Bilbo SD, Brown AS, Hsiao EY, McAllister AK, Meyer U et al. Maternal immune activation: reporting guidelines to improve the rigor, reproducibility, and transparency of the model. Neuropsychopharmacology 2019; 44(2): 245–258. [PubMed: 30188509]
49. Shi Y, Budin F, Yapuncich E, Rumple A, Young JT, Payne C et al. UNC-Emory Infant Atlases for Macaque Brain Image Analysis: Postnatal Brain Development through 12 Months. Front Neurosci 2016; 10: 617. [PubMed: 28119564]
50. Wang J, Vachet C, Rumple A, Gouttard S, Ouziel C, Perrot E et al. Multi-atlas segmentation of subcortical brain structures via the AutoSeg software pipeline. Front Neuroinform 2014; 8: 7. [PubMed: 24567717]
51. Cherel M, Budin F, Prastawa M, Gerig G, Lee K, Buss C et al. Automatic Tissue Segmentation of Neonate Brain MR Images with Subject-specific Atlases. Proc SPIE Int Soc Opt Eng 2015; 9413.
52. Styner M, Knickmeyer R, Joshi S, Coe C, Short S, Gilmore J. Automatic Brain Segmentation in Rhesus Monkeys. Proceedings of SPIE - The International Society for Optical Engineering 2007; 6512.
53. Oguz I, Farzinfar M, Matsui J, Budin F, Liu Z, Gerig G et al. DTIPrep: quality control of diffusion-weighted images. Front Neuroinform 2014; 8: 4. [PubMed: 24523693]
54. Andersson JL, Skare S, Ashburner J. How to correct susceptibility distortions in spin-echo echo-planar images: application to diffusion tensor imaging. Neuroimage 2003; 20(2): 870–888. [PubMed: 14568458]
55. Smith SM, Jenkinson M, Woolrich MW, Beckmann CF, Behrens TE, Johansen-Berg H et al. Advances in functional and structural MR image analysis and implementation as FSL. Neuroimage 2004; 23 Suppl 1: S208–219. [PubMed: 15501092]
56. Andersson JLR, Sotiropoulos SN. An integrated approach to correction for off-resonance effects and subject movement in diffusion MR imaging. Neuroimage 2016; 125: 1063–1078. [PubMed: 26481672]
57. Garyfallidis E, Brett M, Amirbekian B, Rokem A, van der Walt S, Descoteaux M et al. Dipy, a library for the analysis of diffusion MRI data. Front Neuroinform 2014; 8: 8. [PubMed: 24600385]
58. Hoy AR, Koay CG, Kecskemeti SR, Alexander AL. Optimization of a free water elimination two-compartment model for diffusion tensor imaging. Neuroimage 2014; 103: 323–333. [PubMed: 25271843]
59. Avants BB, Epstein CL, Grossman M, Gee JC. Symmetric diffeomorphic image registration with cross-correlation: evaluating automated labeling of elderly and neurodegenerative brain. Med Image Anal 2008; 12(1): 26–41. [PubMed: 17659998]
60. Avants BB, Tustison NJ, Song G, Cook PA, Klein A, Gee JC. A reproducible evaluation of ANTs similarity metric performance in brain image registration. Neuroimage 2011; 54(3): 2033–2044. [PubMed: 20851191]
61. Piontkewitz Y, Arad M, Weiner I. Abnormal trajectories of neurodevelopment and behavior following in utero insult in the rat. Biol Psychiatry 2011; 70(9): 842–851. [PubMed: 21816387]
62. Willette AA, Lubach GR, Knickmeyer RC, Short SJ, Styner M, Gilmore JH et al. Brain enlargement and increased behavioral and cytokine reactivity in infant monkeys following acute prenatal endotoxemia. Behav Brain Res 2011; 219(1): 108–115. [PubMed: 21192986]
63. Crum WR, Sawiak SJ, Chege W, Cooper JD, Williams SCR, Vernon AC. Evolution of structural abnormalities in the rat brain following in utero exposure to maternal immune activation: A longitudinal in vivo MRI study. Brain Behav Immun 2017; 63: 50–59. [PubMed: 27940258]
64. Drazanova E, Ruda-Kucerova J, Kratka L, Horska K, Demlova R, Starcuk Z Jr. et al. Poly(I:C) model of schizophrenia in rats induces sex-dependent functional brain changes detected by MRI that are not reversed by aripiprazole treatment. Brain Res Bull 2018; 137: 146–155. [PubMed: 29155259]
65. Laird NM, Ware JH. Random-effects models for longitudinal data. Biometrics 1982; 38(4): 963–974. [PubMed: 7168798]
66. Hurvich CM, Tsai CL. Regression and Time-Series Model Selection in Small Samples. Biometrika 1989; 76(2): 297–307.
67. Akaike H Likelihood of a Model and Information Criteria. J Econometrics 1981; 16(1): 3–14.

68. Burnham KP, Anderson DR. Multimodel inference - understanding AIC and BIC in model selection. Sociol Method Res 2004; 33(2): 261–304.
69. Nakagawa S, Cuthill IC. Effect size, confidence interval and statistical significance: a practical guide for biologists. Biol Rev Camb Philos Soc 2007; 82(4): 591–605. [PubMed: 17944619]
70. Fatemi SH, Reutiman TJ, Folsom TD, Huang H, Oishi K, Mori S et al. Maternal infection leads to abnormal gene regulation and brain atrophy in mouse offspring: implications for genesis of neurodevelopmental disorders. Schizophr Res 2008; 99(1–3): 56–70. [PubMed: 18248790]
71. Lyall AE, Pasternak O, Robinson DG, Newell D, Trampush JW, Gallego JA et al. Greater extracellular free-water in first-episode psychosis predicts better neurocognitive functioning. Mol Psychiatry 2017.
72. Fatemi SH, Emamian ES, Kist D, Sidwell RW, Nakajima K, Akhter P et al. Defective corticogenesis and reduction in Reelin immunoreactivity in cortex and hippocampus of prenatally infected neonatal mice. Mol Psychiatry 1999; 4(2): 145–154. [PubMed: 10208446]
73. Meyer U, Nyffeler M, Schwendener S, Knuesel I, Yee BK, Feldon J. Relative prenatal and postnatal maternal contributions to schizophrenia-related neurochemical dysfunction after in utero immune challenge. Neuropsychopharmacology 2008; 33(2): 441–456. [PubMed: 17443130]
74. Wischhof L, Irrsack E, Dietz F, Koch M. Maternal lipopolysaccharide treatment differentially affects 5-HT(2A) and mGlu2/3 receptor function in the adult male and female rat offspring. Neuropharmacology 2015; 97: 275–288. [PubMed: 26051401]
75. Zhang Z, van Praag H. Maternal immune activation differentially impacts mature and adult-born hippocampal neurons in male mice. Brain Behav Immun 2015; 45: 60–70. [PubMed: 25449671]
76. Harvey L, Boksa P. A stereological comparison of GAD67 and reelin expression in the hippocampal stratum oriens of offspring from two mouse models of maternal inflammation during pregnancy. Neuropharmacology 2012; 62(4): 1767–1776. [PubMed: 22178614]
77. Nouel D, Burt M, Zhang Y, Harvey L, Boksa P. Prenatal exposure to bacterial endotoxin reduces the number of GAD67- and reelin-immunoreactive neurons in the hippocampus of rat offspring. European neuropsychopharmacology : the journal of the European College of Neuropsychopharmacology 2012; 22(4): 300–307. [PubMed: 21889316]
78. Coiro P, Padmashri R, Suresh A, Spartz E, Pendyala G, Chou S et al. Impaired synaptic development in a maternal immune activation mouse model of neurodevelopmental disorders. Brain Behav Immun 2015; 50: 249–258. [PubMed: 26218293]
79. Richetto J, Chesters R, Cattaneo A, Labouesse MA, Gutierrez AMC, Wood TC et al. Genome-Wide Transcriptional Profiling and Structural Magnetic Resonance Imaging in the Maternal Immune Activation Model of Neurodevelopmental Disorders. Cereb Cortex 2017; 27(6): 3397–3413. [PubMed: 27797829]
80. Smith SE, Li J, Garbett K, Mirnics K, Patterson PH. Maternal immune activation alters fetal brain development through interleukin-6. J Neurosci 2007; 27(40): 10695–10702. [PubMed: 17913903]
81. Estes ML, Prendergast K, MacMahon JA, Cameron S, Aboubechara JP, Farrelly K et al. Baseline immunoreactivity before pregnancy and poly(I:C) dose combine to dictate susceptibility and resilience of offspring to maternal immune activation. Brain Behav Immun 2020; 88: 619–630. [PubMed: 32335198]
82. Garay PA, Hsiao EY, Patterson PH, McAllister AK. Maternal immune activation causes age- and region-specific changes in brain cytokines in offspring throughout development. Brain Behav Immun 2013; 31: 54–68. [PubMed: 22841693]
83. Cassidy CM, Carpenter KM, Konova AB, Cheung V, Grassetti A, Zecca L et al. Evidence for Dopamine Abnormalities in the Substantia Nigra in Cocaine Addiction Revealed by Neuromelanin-Sensitive MRI. Am J Psychiatry 2020; 177(11): 1038–1047. [PubMed: 32854531]
84. Bauman MD, Van de Water J. Translational opportunities in the prenatal immune environment: Promises and limitations of the maternal immune activation model. Neurobiol Dis 2020; 141: 104864. [PubMed: 32278881]
85. Malkova NV, Yu CZ, Hsiao EY, Moore MJ, Patterson PH. Maternal immune activation yields offspring displaying mouse versions of the three core symptoms of autism. Brain Behav Immun 2012; 26(4): 607–616. [PubMed: 22310922]

86. Scheffler F, Kilian S, Chiliza B, Asmal L, Phahladira L, du Plessis S et al. Effects of cannabis use on body mass, fasting glucose and lipids during the first 12months of treatment in schizophrenia spectrum disorders. Schizophr Res 2018; 199: 90–95. [PubMed: 29519756]

87. Coiro P, Pollak DD. Sex and gender bias in the experimental neurosciences: the case of the maternal immune activation model. Transl Psychiatry 2019; 9(1): 90. [PubMed: 30765690]

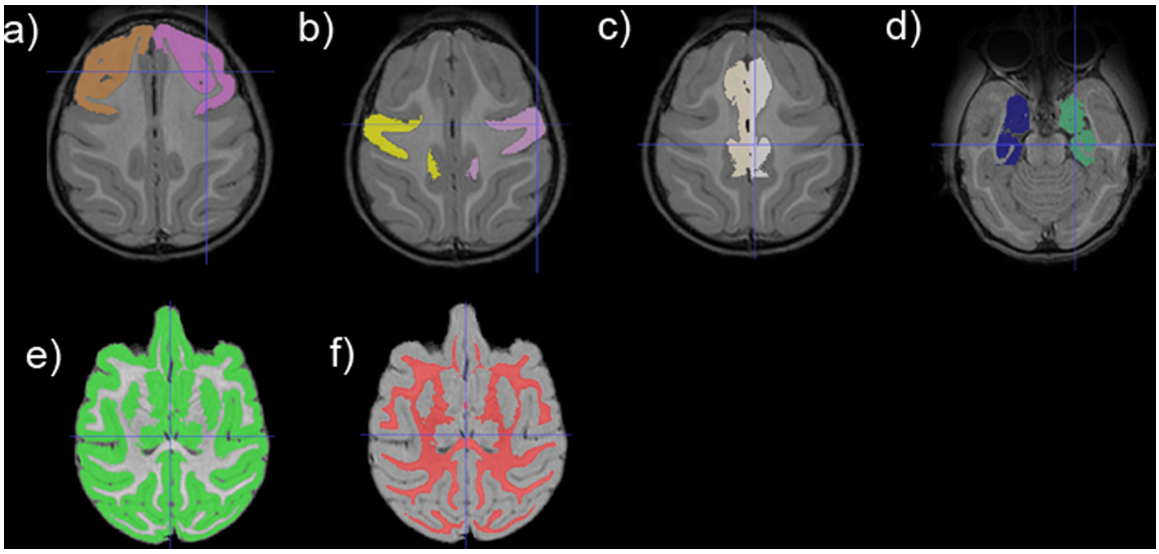

Figure 1:
Depiction of regions of interest: a) prefrontal, b) frontal, c) cingulate, d) temporal limbic, e) whole-brain gray matter, and f) whole-brain white matter.

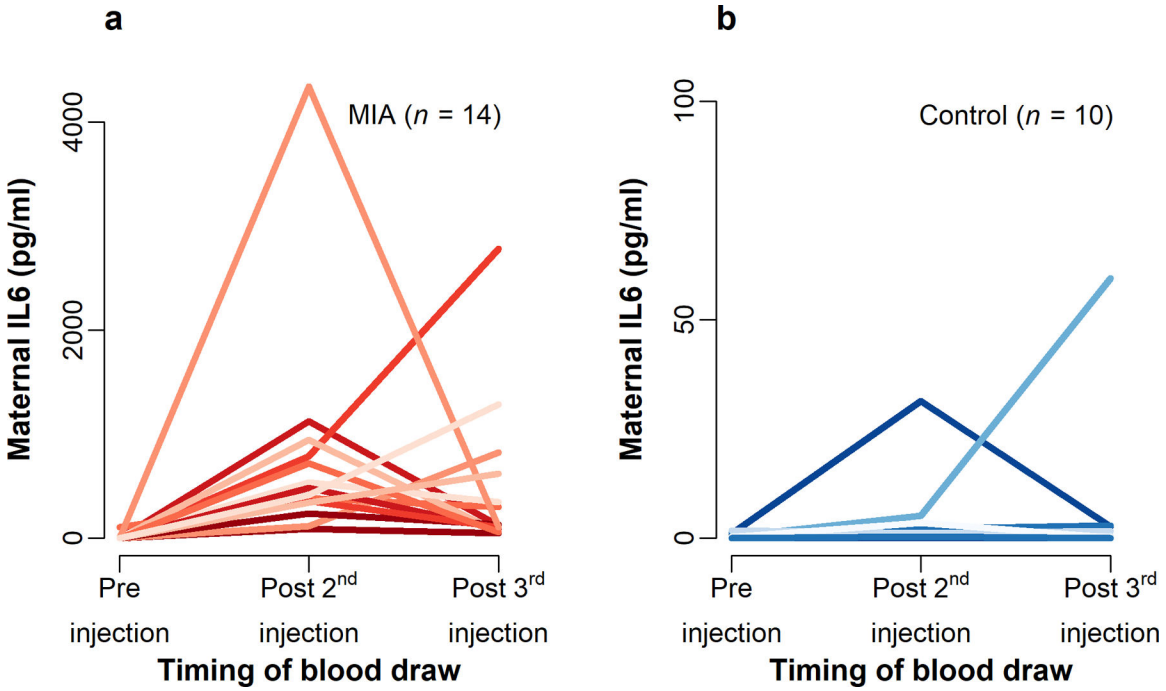

Figure 2:

Depiction of peripheral blood IL-6 response in MIA-exposed (a) and control dams (b) after PolyIC:LC or saline injection, respectively. To allow the plotting of both groups on the same figure, the y-axes ranges are different for the two groups.

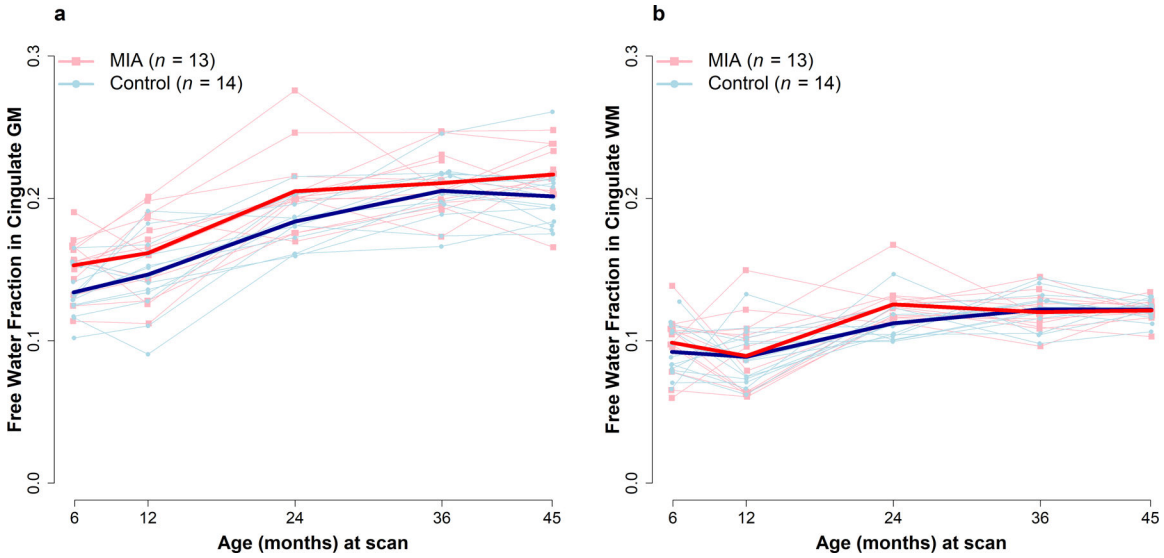

Figure 3:

Free water fraction in cingulate gray (a) and white (b) matter across time in MIA-exposed (red) and Control (blue) offspring.

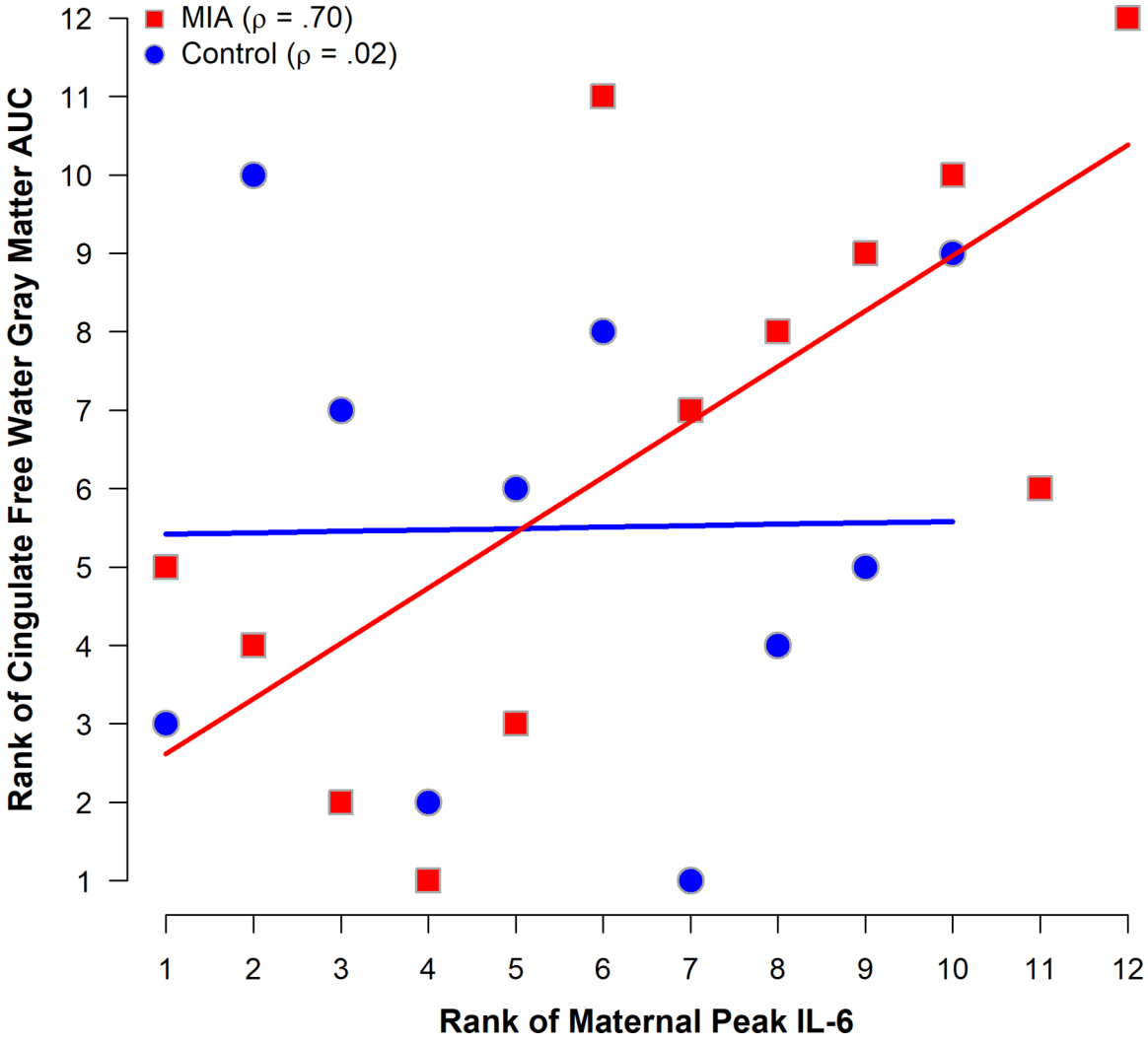

Figure 4:

Correlations between the summary measure of free mater fraction in cingulate gray matter and maternal immune response in MIA-exposed and Control offspring. The graph shows rank-transformed data and Spearman's rank correlations (ρ).

Table 1.

Summary of the free water (FW) measures from 6 to 45 months in MIA-exposed and Control offspring.

	Fractional Anisotropy		White Matter FW		Gray Matter FW	
	MIA (*n* = 13)	**Control (*n* = 14)**	**MIA (*n* = 13)**	**Control (*n* = 14)**	**MIA (*n* = 13)**	**Control (*n* = 14)**
Whole-brain Measures, *Mean* (*SD*)						
6 months	0.352 (0.015)	0.355 (0.010)	0.129 (0.011)	0.121 (0.011)	0.149 (0.016)	0.138 (0.014)
12 months	0.380 (0.015)	0.378 (0.014)	0.128 (0.018)	0.123 (0.016)	0.157 (0.022)	0.152 (0.020)
24 months	0.421 (0.014)	0.427 (0.012)	0.162 (0.007)	0.159 (0.006)	0.203 (0.019)	0.194 (0.016)
36 months	0.436 (0.014)	0.442 (0.011)	0.166 (0.011)	0.165 (0.005)	0.213 (0.018)	0.211 (0.018)
45 months[a]	0.447 (0.013)	0.451 (0.011)	0.168 (0.009)	0.165 (0.007)	0.217 (0.016)	0.208 (0.021)
Prefrontal Measures, *Mean* (*SD*)						
6 months	0.367 (0.024)	0.372 (0.013)	0.087 (0.010)	0.080 (0.015)	0.118 (0.016)	0.114 (0.016)
12 months	0.376 (0.022)	0.374 (0.019)	0.080 (0.017)	0.081 (0.017)	0.124 (0.023)	0.121 (0.018)
24 months	0.417 (0.021)	0.412 (0.012)	0.131 (0.012)	0.121 (0.013)	0.174 (0.018)	0.166 (0.017)
36 months	0.423 (0.017)	0.421 (0.013)	0.130 (0.011)	0.129 (0.015)	0.179 (0.020)	0.184 (0.018)
45 months[a]	0.429 (0.016)	0.429 (0.015)	0.129 (0.008)	0.128 (0.011)	0.188 (0.018)	0.182 (0.020)
Frontal Measures, *Mean* (*SD*)						
6 months	0.400 (0.012)	0.399 (0.013)	0.107 (0.015)	0.099 (0.014)	0.138 (0.015)	0.132 (0.015)
12 months	0.420 (0.017)	0.417 (0.018)	0.100 (0.020)	0.099 (0.015)	0.142 (0.019)	0.139 (0.020)
24 months	0.463 (0.017)	0.464 (0.014)	0.142 (0.007)	0.139 (0.006)	0.180 (0.015)	0.180 (0.013)
36 months	0.475 (0.015)	0.477 (0.014)	0.146 (0.010)	0.149 (0.006)	0.186 (0.020)	0.189 (0.016)
45 months[a]	0.484 (0.012)	0.481 (0.016)	0.149 (0.007)	0.147 (0.007)	0.190 (0.015)	0.182 (0.016)
Cingulate Measures, *Mean* (*SD*)						
6 months	0.373 (0.023)	0.381 (0.015)	0.099 (0.021)	0.092 (0.018)	0.153 (0.021)	0.134 (0.018)
12 months	0.389 (0.032)	0.390 (0.020)	0.089 (0.028)	0.089 (0.020)	0.162 (0.029)	0.147 (0.027)
24 months	0.424 (0.019)	0.422 (0.023)	0.125 (0.014)	0.112 (0.013)	0.205 (0.029)	0.184 (0.017)
36 months	0.431 (0.020)	0.440 (0.018)	0.120 (0.013)	0.122 (0.013)	0.211 (0.022)	0.205 (0.020)
45 months[a]	0.432 (0.016)	0.444 (0.023)	0.121 (0.008)	0.122 (0.007)	0.217 (0.022)	0.201 (0.022)
Temporal Limbic Measures, *Mean* (*SD*)						
6 months	0.347 (0.024)	0.358 (0.020)	0.141 (0.010)	0.138 (0.013)	0.184 (0.013)	0.176 (0.012)

	Fractional Anisotropy		White Matter FW		Gray Matter FW	
	MIA (n = 13)	Control (n = 14)	MIA (n = 13)	Control (n = 14)	MIA (n = 13)	Control (n = 14)
12 months	0.362 (0.021)	0.368 (0.016)	0.149 (0.016)	0.145 (0.020)	0.187 (0.021)	0.185 (0.020)
24 months	0.377 (0.020)	0.390 (0.020)	0.167 (0.021)	0.167 (0.013)	0.215 (0.018)	0.207 (0.013)
36 months	0.403 (0.018)	0.405 (0.019)	0.179 (0.020)	0.179 (0.016)	0.216 (0.016)	0.223 (0.016)
45 months[a]	0.421 (0.019)	0.430 (0.024)	0.181 (0.013)	0.180 (0.014)	0.226 (0.013)	0.223 (0.016)

Abbreviations: MIA, maternal immune activation; SD, standard deviation. Data are missing for:

[a] n = 1 MIA.

Table 2.

Summary of the linear mixed-effects models[a] examining trajectories of free water (FW) measures from 6 to 45 months in MIA-exposed and Control offspring

	Fractional Anisotropy		White Matter FW		Gray Matter FW	
Model Term	**Estimate (*SE*)**	***P*-value**	**Estimate (*SE*)**	***P*-value**	**Estimate (*SE*)**	***P*-value**
Whole-Brain Measures						
Intercept	91.80 (0.64)	< 0.001	32.80 (0.35)	< 0.001	40.32 (0.75)	< 0.001
MIA (vs. Control)	−0.30 (0.42)	0.48	0.39 (0.22)	0.08	0.77 (0.48)	0.12
Linear	7.91 (0.16)	< 0.001	3.98 (0.24)	< 0.001	6.26 (0.29)	< 0.001
Quadratic	−2.05 (0.15)	< 0.001	−1.20 (0.13)	< 0.001	−1.87 (0.26)	< 0.001
Cubic	0.24 (0.15)	0.10	−0.61 (0.19)	0.002	−0.59 (0.26)	0.03
Quartic	0.50 (0.15)	0.001	0.98 (0.19)	< 0.001	0.76 (0.26)	0.004
Prefrontal Measures						
Intercept	89.62 (0.82)	< 0.001	24.10 (0.44)	< 0.001	34.23 (0.71)	< 0.001
MIA (vs. Control)	0.24 (0.53)	0.65	0.35 (0.29)	0.24	0.36 (0.45)	0.43
Linear	5.30 (0.22)	< 0.001	4.50 (0.23)	< 0.001	6.29 (0.30)	< 0.001
Quadratic	−1.23 (0.20)	< 0.001	−1.58 (0.23)	< 0.001	−1.68 (0.29)	< 0.001
Cubic	−0.35 (0.20)	0.09	−0.95 (0.23)	< 0.001	−0.70 (0.29)	0.02
Quartic	1.00 (0.20)	< 0.001	1.45 (0.23)	< 0.001	1.09 (0.29)	< 0.001
Frontal Measures						
Intercept	100.15 (0.76)	< 0.001	28.45 (0.36)	< 0.001	36.81 (0.69)	< 0.001
MIA (vs. Control)	0.06 (0.49)	0.90	0.09 (0.22)	0.67	0.25 (0.45)	0.58
Linear	7.08 (0.16)	< 0.001	4.45 (0.25)	< 0.001	4.79 (0.27)	< 0.001
Quadratic	−2.01 (0.15)	< 0.001	−1.19 (0.19)	< 0.001	−1.71 (0.24)	< 0.001
Cubic	−0.06 (0.15)	0.68	−0.93 (0.19)	< 0.001	−0.63 (0.24)	0.01
Quartic	0.68 (0.15)	< 0.001	1.23 (0.19)	< 0.001	0.87 (0.24)	< 0.001
Cingulate Measures						
Intercept	92.93 (0.99)	< 0.001	24.26 (0.43)	< 0.001	38.93 (1.00)	< 0.001
MIA (vs. Control)	−0.58 (0.64)	0.37	0.13 (0.25)	0.61	1.55 (0.66)	0.03
Linear	5.34 (0.28)	< 0.001	2.76 (0.28)	< 0.001	5.92 (0.34)	< 0.001
Quadratic	−1.42 (0.28)	< 0.001	−0.75 (0.27)	0.006	−1.67 (0.32)	< 0.001
Cubic	–	–	−0.74 (0.31)	0.02	−0.54 (0.31)	0.09
Quartic	–	–	1.06 (0.33)	0.002	0.63 (0.31)	0.048
Temporal Limbic Measures						
Intercept	87.27 (0.98)	< 0.001	36.21 (0.59)	< 0.001	45.37 (0.67)	< 0.001
MIA (vs. Control)	−0.86 (0.64)	0.19	0.15 (0.38)	0.70	0.29 (0.44)	0.52
Linear	5.87 (0.25)	< 0.001	3.64 (0.26)	< 0.001	3.90 (0.25)	< 0.001
Quadratic	–	–	-0.75 (0.26)	0.004	−0.75 (0.24)	0.002
Cubic	–	–	–	–	−0.22 (0.24)	0.35
Quartic	–	–	–	–	0.46 (0.24)	0.053

Abbreviations: MIA, maternal immune activation, *SE* = standard error.

[a]Mixed-effects linear regression fitted to13 MIA-exposed (n = 1 missing data at 45 months) and 14 control offspring using up to fourth-order orthogonal polynomial models. To aid model convergence, all outcomes were rescaled (by multiplying with 100). Random intercepts and slopes were used to account for within-animal dependence. Initial models included fixed effects for the group (MIA vs. control), linear, quadratic, cubic, and quartic orthogonal polynomials for age at scan (measured in years), and interactions between the group and the effects of age. Higher-degree polynomial and interaction terms were sequentially removed, and models were compared to identify the reported models using the lowest corrected Akaike information criterion. Note that in this approach, the intercept term does not stand for the y-intercept but rather is the average y-value of the modeled curve, the linear term reflects a monotonic change in free water, and the quadratic term reflects an increase following a decrease in free water. The cubic and quartic terms tend to capture minor details in the curve's tails.